ELSEVIER

Available online at www.sciencedirect.com

SCIENCE DIRECT®

Journal of Molecular Structure 780–781 (2006) 115–123

Journal of
MOLECULAR
STRUCTURE

www.elsevier.com/locate/molstruc

High-resolution infrared study of the ν_1 and ν_3 bands, and the equilibrium structure of AsD_3

O.N. Ulenikov[a,*], E.S. Bekhtereva[a], Yu. B. Yuhnik[a], H. Bürger[b]

[a] *Laboratory of Molecular Spectroscopy, Physics Department, Tomsk State University, Tomsk, 634050, Russian Federation*
[b] *Anorganische Chemie, FB C, Bergische Universität, D-42097 Wuppertal, Germany*

Received 11 April 2005; revised 18 May 2005; accepted 19 May 2005
Available online 13 October 2005

Abstract

The infrared spectrum of the AsD_3 molecule has been measured in the region of the stretching fundamental bands on a Fourier transform spectrometer with a resolution of $0.0027\ cm^{-1}$ and analyzed for the first time. More than 3300 normally allowed and in addition more than 900 forbidden, but perturbation-allowed transitions with $J^{upper}_{max} = 28$ have been assigned to the bands ν_1 and ν_3. An effective Hamiltonian was used which takes into account the resonance interactions between the states (1000) and (0010). A set of 50 (26 diagonal and 24 resonance) refined spectroscopic parameters was obtained from the fit which reproduces the 1229 initial 'experimental' upper state ro-vibrational energies with an *rms* deviation of $0.00024\ cm^{-1}$. The transition moment ratio $|\mu_1{:}\mu_3|$ was determined to be 1.2 ± 0.05, and the intensity perturbation $\mu_1\ \xi^y_{13}\ \mu_3$ found to be negative. The equilibrium values of the bond length $r^e_{As\text{–}D} = 1.51130(11)$ A and interbond angle $\alpha^e_{D\text{–}As\text{–}D} = 92.0775(40)^\circ$ were determined from the values of the rotational parameters of the ground state and the four fundamental bands.

Keywords: Vibration-rotation spectra; AsD3 molecule; Stretching fundamentals; Spectroscopic parameters; Equilibrium structure

1. Introduction

The heavier homologues of ammonia, namely PH_3, AsH_3, SbH_3, and BiH_3 are subjects of large spectroscopic interest for a number of reasons. On the one hand, the study of their spectra is important for some astrophysical applications because some of these were detected in the atmospheres of the giant planets Saturn and Jupiter [1–6]. On the other hand, these molecules are of interest from a theoretical point of view because they all are light, near spherical symmetric top pyramidal molecules with some special properties. As a consequence, numerous spectroscopic effects and peculiarities which are inherent to molecules of this kind should be particularly pronounced in their spectra. An additional interest in the spectroscopic study of the PH_3, AsH_3, SbH_3, and BiH_3 molecules arises from the fact that they can be considered as local mode molecules, see [7–10] and references therein. Both the local mode properties and the conditions of their breakdown can be and have been analyzed in the stretching bands and their overtones of PH_3, AsH_3, SbH_3, and BiH_3.

Whenever it is desirable to obtain as complete as possible spectroscopic information on a target molecule, the study of isotopic varieties of such a species is an efficient means to gather valuable additional information. The larger the mass ratio of the isotopically labeled variety with regard to the reference 'mother' molecule is, the more pronounced are the apparent isotopic effects on the spectrum and the rovibrational energy pattern. The greater the variety of isotopic substitution, the more effects can be evaluated and analyzed in detail. Accordingly, the study of deuterated species of a hydride molecule is the most efficient strategy because the ratio $(m_D - m_H)/m_H$ is the largest conceivable for stable isotopes. All the above-mentioned reasons clearly suggest that a high-resolution spectroscopic study of the stretching fundamentals of the totally deuterated species of arsine, AsD_3, which is presented in this contribution, is suitable and timely.

The pure rotational spectra of the AsD_3 molecule have been extensively analyzed earlier both in the millimeter and submillimeter wave regions [11–14]. As to the infrared (IR) spectra, there are only two studies which have come to our

---

[*] Corresponding author.
E-mail address: ulenikov@phys.tsu.ru (O.N. Ulenikov).

0022-2860/$ - see front matter © 2005 Elsevier B.V. All rights reserved.
doi:10.1016/j.molstruc.2005.05.054

attention. One of them is the elder low-resolution ($\sim$0.3 cm^{-1}) study of the ν_1 and ν_3 bands [15]. The other one is our recent high-resolution IR study and analysis of the bending fundamentals ν_2 and ν_4, Ref. [16]. In that study also the ground state parameters were obtained making use of a large number of forbidden, but perturbation-allowed lines.

In the present contribution, we report on the results of the first high-resolution spectroscopic investigation of the two strongly interacting stretching fundamentals ν_1 and ν_3 of AsD_3. The respective experimental details are given in Section 2. Section 3 presents briefly the Hamiltonian used in the fit of the rotational–vibrational energies extracted from the experimental data. Assignments of the measured transitions are gathered in Section 4. Section 5 discusses the results of our analysis. Some remarks concerning the equilibrium structural parameters derived from the former [16] and the present results are presented in Section 6.

2. Experimental details

A sample of AsD_3 was prepared from $AsCl_3$ and $LiAlD_4$ as reported in Ref. [16]. A high-resolution IR spectrum was recorded at Wuppertal with a Bruker 120 HR interferometer: This was equipped with a Globar source, a KBr beamsplitter, and an MCT 800 detector. A cell measuring 280 mm in length and outfitted with KBr windows was employed, and a pressure of 60 Pa adjusted. The resolution (1/maximum optical path difference) chosen was 0.0027 cm^{-1}. The region 1200–2050 cm^{-1} was recorded, and in total 400 scans coadded. Calibration was done using lines of residual H_2O in the interferometer. These were selected from the 1380–1440 and 1615–1680 cm^{-1} ranges and were taken from Ref. [17] and corrected according Ref. [18]. Wavenumber precision is about 0.0002 cm^{-1}, wavenumber accuracy better than 0.0005 cm^{-1}. Fig. 1 presents the overview of the ν_1 and ν_3 band spectrum in the region of 1400–1650 cm^{-1}.

3. Theoretical background

The AsD_3 is an oblate symmetric top with a D–As–D bond angle close to 90°. Its stretching fundamental bands ν_1 and ν_3 are close to each other, with band centers at 1523.20 and 1533.76 cm^{-1}, respectively (see below). So, one can expect an appearance in the spectrum of strong Coriolis-type interactions between the states (1000) and (0010). The (1000) and (0010) states are located at about 100 cm^{-1} higher than the first overtones of the bending fundamentals ν_2 and ν_4 (654.41 and 714.34 cm^{-1}, respectively [16]), and therefore perturbations from these overtones will become relevant probably only for sufficiently high ro-vibrational states with $J \geq 25$–27.

In the present study, we therefore adopt a Hamiltonian model derived earlier in [7,19] on the basis of the symmetry properties of the molecule. This takes into account any kind of effects, which can be produced by the Coriolis interaction between the A_1- and E-type vibrational states of a symmetric top molecule. This Hamiltonian has the form of the effective operator

$$H^{v.-r.} = \sum_{v,v'} H^{vv'}, \tag{1}$$

where the summation extends to the A_1 and E vibrational states ((1000) and (0010) in our case). The diagonal operators H^{vv} describe rotational structures of corresponding vibrational states. The nondiagonal operator $H^{A,E}$ describes the Coriolis-type resonance interactions between the states $|v\rangle \equiv (1000)$ and $|v'\rangle \equiv (0010)$. In the case of symmetric vibrational states (A_1 symmetry), the $H^{A_1A_1}$ operators have the form

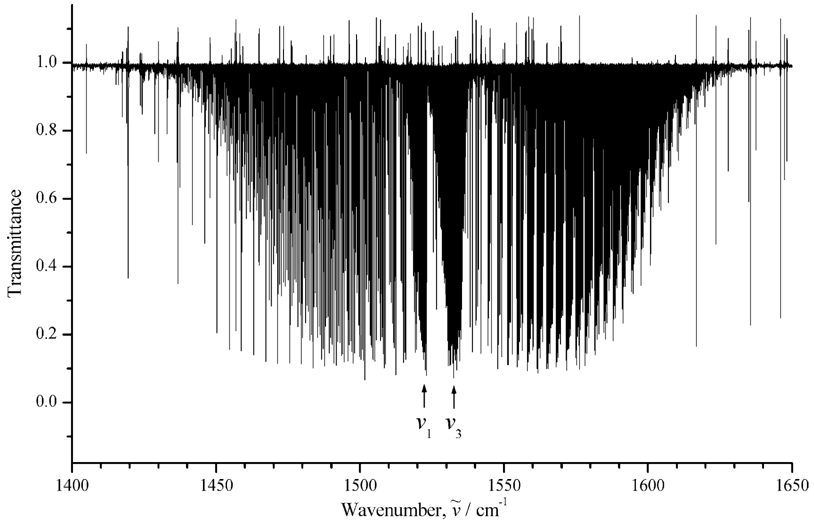

Fig. 1. Survey spectrum of AsD_3 in the region of 1400–1650 cm^{-1}. The centers of the bands ν_1 and ν_3 located in this region are denoted. Some strong lines both on the left and right hand sides of the spectrum belong to water present in the interferometer. The weak $2\nu_4$ band can be seen close to 1400 cm^{-1}.

$$\begin{aligned} H^{A_1,A_1} = |A_1\rangle\langle A_1|\{&E^a + B^a(J_x^2+J_y^2) + C^aJ_z^2 - D_J^2J^4 \\ &- D^a_{JK}J^2J_z^2 - D^a_KJ_z^4 + H^a_JJ^6 + H^a_{JK}J^4J_z^2 \\ &+ H^a_{KJ}J^2J_z^4 + H^a_KJ_z^6 + L^a_JJ^8 + \ldots \\ &+ [(\varepsilon^{\prime a}J_z + \varepsilon^{\prime a}_JJ_zJ^2 + \varepsilon^{\prime a}_KJ_z^3 + \ldots),(J_+^3+J_-^3)]_+ \\ &+ h^{\prime a}(J_+^6+J_-^6) + \ldots\} \end{aligned} \tag{2}$$

Here B^a, C^a, D^a_J, D^a_{JK}, D^a_K, H^a_J, H^a_{JK} H^a_{KJ}, H^a_K, L^a_J, … are the rotational and centrifugal distortion parameters, respectively. Operators $(J_+^3+J_-^3)$ connect rotational states $|JK\rangle$ and $|JK'\rangle$ with different values of the quantum numbers K, namely $\Delta K = K - K' = \pm 3$. They account, in particular, for the A_1/A_2 splittings of $K=3$ levels, and J_+ and J_- operators have the form of $J_\pm = J_x \mp iJ_y$. Parameters $\varepsilon^{\prime a}_J$ and $\varepsilon^{\prime a}_K$ describe the J and K dependencies of the main $\varepsilon^{\prime a}$ parameter. The expression $[\ldots,\ldots]_+$ denotes an anticommutator.

For doubly degenerate vibrational states (E symmetry) the H^{EE} operator is

$$H^{\mathrm{EE}} = H_1^{\mathrm{EE}} + H_2^{\mathrm{EE}} + H_3^{\mathrm{EE}}, \tag{3}$$

where

$$\begin{aligned} H_1^{\mathrm{EE}} = (|E_1\rangle\langle E_1| + |E_2\rangle\langle E_2|)\{&E^e + B^e(J_x^2+J_y^2) \\ &+ C^eJ_z^2 - D^e_JJ^4 - D^e_{JK}J^2J_z^2 - D^e_KJ_z^4 + H^e_JJ^6 \\ &+ H^e_{JK}J^4J_z^2 + H^2_{KJ}J^2J_z^4 + H^e_KJ_z^6 + L^e_JJ^8 + \ldots \\ &+ [(\varepsilon^{\prime e}J_z + \varepsilon^{\prime e}_JJ_zJ^2 + \varepsilon^{\prime e}_KJ_z^3 + \ldots),(J_+^3+J_-^3)]_+ \end{aligned} \tag{4}$$

$$\begin{aligned} H_2^{\mathrm{EE}} = (|E_1\rangle\langle E_2| - |E_2\rangle\langle E_1|)\{&2(C\zeta)J_z + \eta_JJ_zJ^2 + \eta_KJ_z^3 \\ &+ \eta_{JJ}J_zJ^4 + \eta_{JK}J_z^3J^2 + \eta_{KK}J_z^5 + \eta_{JJJ}J_zJ^6 \\ &+ \eta_{JJK}J_z^3J^4 + \eta_{JKK}J_z^5J^2 + \eta_{KKK}J_z^7 + \ldots\}, \end{aligned} \tag{5}$$

and

$$\begin{aligned} H_3^{\mathrm{EE}} = (|E_2\rangle\langle E_2| - |E_1\rangle\langle E_1|)\{&[iA,(J_+-J_-)]_+ \\ &+ [B,(J_++J_-)]_+ + [C,(J_+^2+J_-^2)]_+ \\ &+ [iD,(J_-^2-J_+^2)]_+ + [F,(J_+^4+J_-^4)]_+ \\ &+ [iG,(J_-^4-J_+^4)]_+\} + (|E_1\rangle\langle E_2| + |E_2\rangle\langle E_1|) \\ &\times\{[A,(J_++J_-)]_+ + [iB,(J_--J_+)]_+ \\ &+ [iC,(J_+^2-J_-^2)]_+ + [D,(J_+^2+J_-^2)]_+ \\ &+ [iF,(J_+^4-J_-^4)]_+ + [G,(J_+^4+J_-^4)]_+\}, \end{aligned} \tag{6}$$

$$\begin{aligned} A &= \frac{1}{2}\alpha + \frac{1}{2}\alpha_JJ^2 + \alpha_KJ_z^2 + \frac{1}{2}\alpha_{JJ}J^4 + \alpha_{JK}J^2J_z^2 \\ &\quad + \alpha_{KK}J_z^4 + \cdots + \alpha_{JJK}J^4J_z^2 + \alpha_{JKK}J^2J_z^4 + \ldots, \\ B &= \beta J_z + \beta_JJ_zJ^2 + \beta_KJ_z^3 + \beta_{JJ}J^4J_z + \beta_{JK}J^2J_z^3 + \ldots, \\ C &= \frac{1}{2}\gamma + \frac{1}{2}\gamma_JJ^2 + \gamma_KJ_z^2 + \frac{1}{2}\gamma_{JJ}J^4 + \gamma_{JK}J^2J_z^2 + \cdots \\ &\quad + \gamma_{JJK}J^4J_z^2 + \ldots, \\ D &= \delta J_z + \delta_JJ_zJ^2 + \delta_KJ_z^3 + \delta_{JJ}J_zJ^4 + \delta_{JK}J^2J_z^3 + \ldots, \\ F &= \frac{1}{2}\kappa + \frac{1}{2}\kappa_JJ_z^2 + \kappa_KJ_z^2 + \frac{1}{2}\kappa_{JJ}J^4 + \kappa_{JK}J^2J_z^2 + \ldots, \\ G &= \theta J_z + \theta_JJ_zJ^2 + \theta_KJ_z^3 + \theta_{JJ}J_zJ^4 + \theta_{JK}J^2J_z^3 + \ldots, \end{aligned} \tag{7}$$

In Eq. (4) the E^{e},B^{e},…, $\varepsilon^{\prime\mathrm{e}}$ parameters have the same meaning as the corresponding ones in Eq. (2) with only one exception: although operators $(J_+^3+J_-^3)$ connect rotational states $|JK\rangle$ and $|JK'\rangle$ with $\Delta K = K - K' = \pm 3$, they do not split A_1/A_2 levels. The operator H_2^{EE} describes the $k-l$ splittings; other type operators, $(J_+^n \pm J_-^n)$, connect rotational states $|JK\rangle$ and $|JK'\rangle$ where $\Delta K = K - K' = \pm n$. Of these, the operators with $n=2m$ provide the $A_1 - A_2$ splittings of energy levels with $K=m$.

Resonance interaction (Coriolis-type) operators which connect vibrational states of different symmetries, A_1 and E have the following form:

$$\begin{aligned} H^{vA_1v'E} = |A_1\rangle\langle E_1|\{&[iA^*,(J_+-J_-)]_+ \\ &+ [B^*,(J_++J_-)]_+ + [C^*,(J_+^2+J_-^2)]_+ \\ &+ [iD^*,(J_-^2-J_+^2)]_+ + [F^*,(J_+^4+J_-^4)]_+ \\ &+ [iG^*,(J_-^4-J_+^4)]_+\} \\ &+ |A_1\rangle\langle E_2|\{[A^*,(J_++J_-)]_+ + [iB^*,(J_--J_+)]_+ \\ &+ [iC^*,(J_+^2-J_-^2)]_+ + [D^*,(J_+^2+J_-^2)]_+ \\ &+ [iF^*,(J_+^4-J_-^4)]_+ + [G^*,(J_+^4+J_-^4)]_+\}. \end{aligned} \tag{8}$$

The operators A^*, B^*,…, etc. can be derived from Eq. (7) by replacing the parameters α, β,… by a^*, β^*,…, etc.

4. Description and assignment of the spectrum

Fig. 1 shows an overview spectrum of the bands ν_1 and ν_3. Although the separation between the ν_1 and ν_3 band centers is only 10.56 cm^{-1}, one can clearly see a pair of well pronounced Q-branches separated from each other. One of them belonging to the ν_1 band consists of ${}^QQ_K(J)$

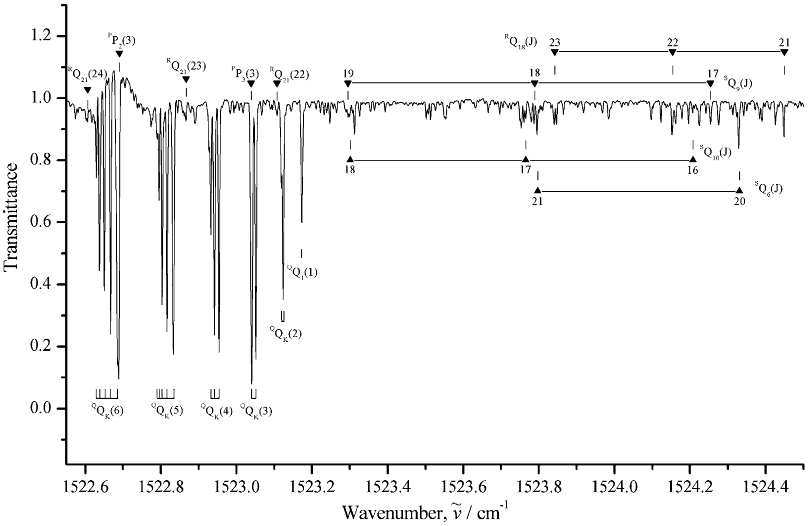

Fig. 2. Small portion of the Q-branchs of the ν_1 band of AsD_3 shown on the left hand side. In addition to the Q-clusters of the ν_1 band, some bunches of denoted weak lines belonging to the ν_3 band are visible. Those on the left hand side are normally allowed transitions and those on the right hand side are perturbation-allowed transitions.

type transitions, Fig. 1 (small fragment of the *Q*-branch is shown also in Fig. 2). The other one, which belongs to the ν_3 band, is composed of overlapping $^{P}Q_K(J)$ and $^{R}Q_K(J)$ transitions. These branches reveal similar intensities and they are both degraded to small wavenumbers. The *P*- and *R*-branches are also clearly visible. But, contrary to the *Q*-branches, they are totally overlapped for the two bands. Strong lines both on the left and right side of the spectrum shown in Fig. 1 belong to water present in the interferometer. In addition the weak $2\nu_4$ band can be detected close to 1400 cm^{-1}.

The $P_K(J)$ and $R_K(J)$ transitions of the ν_1 band have comparable strengths. The regular *J*-cluster structure of the *P*- and *R*-branches is quite prominent and visible in the lower and higher wavenumber regions, respectively, up to $P_K(19)$ and $R_K(17)$ transitions. However, beginning with the $P_K(20)$ and $R_K(18)$ transitions, the regular cluster structure begins to disappear. In this case, both the distances between neighboring lines and the line strengths become irregular. As the further analysis will show, the ro-vibrational structures of the (1000) and (0010) states are reproduced with a high accuracy within the Hamiltonian model of two interacting vibrational states without taking into account the resonance interactions with the first bending overtones and combinational states, at least up to values of $J=25$–27. It means, that the reason for the breakdown of the regular structures of the clusters $P_K(J\geq 20)$ and $R_K(J\geq 18)$ is due to the Coriolis interaction inside the pair (1000)/(0010).

The ν_3 band, a small part of which is illustrated in Fig. 3, is above all characterized by strong $^{R}R_K(J)$ and $^{P}P_K(J)$ transitions. Those of the types $^{P}R_K(J)$ and $^{R}P_K(J)$ are considerably weaker than corresponding $^{R}R_K(J)$ and $^{P}P_K(J)$ ones for smaller values of *J*. However, with increasing *J* (for given *K*), the strengths of $^{R}R_K(J)$ and $^{P}P_K(J)$ transitions decrease considerably faster than those of $^{P}R_K(J)$ and $^{R}P_K(J)$ ones. As a consequence, all transitions in the *R*- and *P*-branches have comparable line strengths, as a rule, for the values of the quantum number $J\geq 19$–20.

In accordance with the symmetry, the selection rules for the strongest ‘allowed’ transitions are:

$$\Delta J=0,\pm 1; \quad \Delta K=0; \quad E\rightarrow E, \quad A_1\leftrightarrow A_2 \quad \text{if } K\neq 0$$

$$\Delta J=\pm 1; \quad \Delta K=0; \quad A_1\leftrightarrow A_2 \quad \text{if } K=0$$

for the parallel band ν_1 and

$$\Delta J=0,\pm 1; \quad \Delta K=\pm 1; \quad E\rightarrow E, \quad A_1\leftrightarrow A_2$$

for the perpendicular band ν_3. However, the conditions $\Delta K=0$ (for parallel bands) and/or $\Delta K\pm 1$ (for perpendicular bands) are not a strict ones. In principle, the presence of resonance interactions can lead to appearance of of so-called ‘forbidden’ transitions with arbitrary values of difference ΔK.

Assignments of lines were made on the basis of the Ground State Combination Differences (GSCD) method, and the ground state energies were calculated with the parameters from [16], model 3. More than 850 and 2450 normally allowed transitions were assigned to the ν_1 and ν_3 bands, respectively (see Table 1). Corresponding ‘experimental’ upper state ro-vibrational energies and their uncertainties Δ, for both vibrational bands were determined from transitions reaching the same upper state and are presented as the supplementary materials [20] in columns 2 and 3 of Tables SM1 and SM2 in units of cm^{-1} and 10^{-4} cm^{-1}, respectively. No Δ value is quoted in columns 3 when the upper energy value was obtained from only one transition.

The presence of strong Coriolis interactions between the states (1000) and (0010) leads in the experimental spectrum to the appearance of numerous ‘forbidden’, but

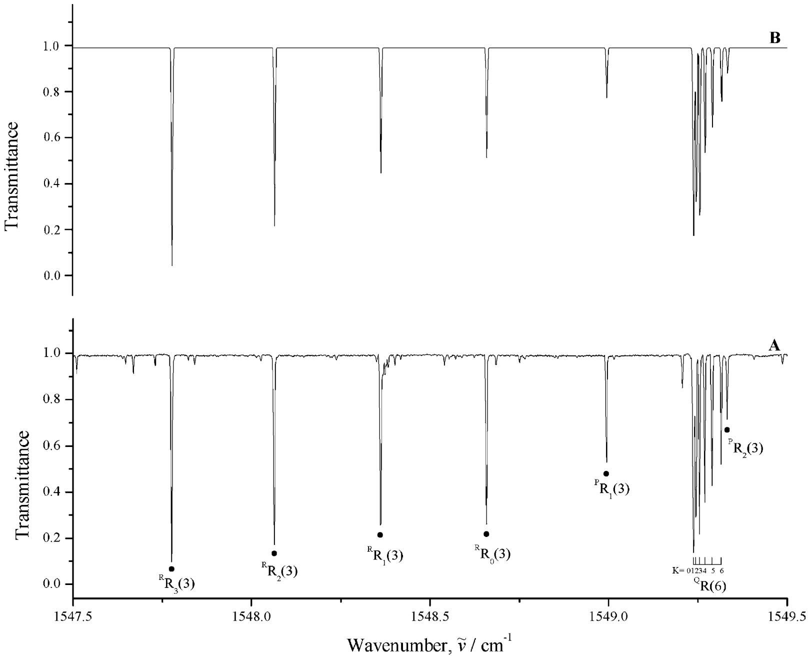

Fig. 3. Detail of the ν_1/ν_3 band spectrum of AsD_3 in the R-branch region. (A) Experimental spectrum. (B) Simulated spectrum. Lines both of the ν_1 and ν_3 bands are labeled.

perturbation-allowed transitions of the $^{S}X_K(J)$ and $^{O}X_K(J)$ ($X=P$, Q, R, $J^{\text{upper}}_{\text{max.}}=25$) types. Indeed we have observed more than 100 'forbidden' transitions in the ν_1 band with $\Delta K=1$ and 2, $J_{\text{max.}}=23$ and $K_{\text{max.}}=14$, and more than 800 in the ν_3 band with $\Delta K=0$ and 2, $J_{\text{max.}}=23$ and $K_{\text{max.}}=18$. These very weak lines did not provide any new upper state energies although they were useful to confirm them by means of GSCD and hereby made them valuable for the data fit. Some of such transitions are illustrated on Fig. 2. There are more 'forbidden' lines than used for the determination of upper state energies but they were blended by other absorptions and therefore not considered 'assigned'.

5. Determination of spectroscopic parameters and discussion

In general, the rotational and centrifugal distortion parameters of vibrationally excited states differ only slightly from those of the ground vibrational state. A preliminary analysis however revealed that the unconstrained fit of the data from Tables SM1 and SM2 considerably changes the values of all rotational and centrifugal distortion parameters in excited states with respect to their ground state values if one tries to fit the levels as noninteracting states. The reason for this behavior is the presence of strong resonance interactions between all levels relevant for this study, which perturb the ro-vibrational structures of the upper states already for small J values. It is known [21] that taking resonance interactions into account can lead to strong correlations (ambiguities) between the rotational parameters and centrifugal distortion coefficients of diagonal blocks of the Hamiltonian (1), on the one hand, and the resonance interaction parameters of nondiagonal blocks, on the other hand. For this reason, some physically justified restrictions limiting such ambiguities should be obeyed. One such possibility is the reduction of the Hamiltonian (see, e.g. [22]). Another physically reasonable assumption is that the values of the centrifugal distortion coefficients of a not too strongly excited vibrational state of a 'rigid' molecule should be close to those of corresponding parameters of the ground vibrational state. Thirdly, it is for the same reason physically meaningful to vary some of the parameters in a controlled manner. Accordingly, a fit procedure may be conceived in such a way that parameters with the same physical meaning belonging to different vibrational states are refined jointly. Therefore, we have varied all H and ϵ' parameters of the (1000) state and constrained at any step of the fit the corresponding H and ϵ' parameters of the (0010) state to exactly the same values. The parameters ε'_J and ε'_K of both vibrational states were constrained to their values in the ground vibrational state. Altogether a set of 26 parameters of the diagonal blocks was used in the fit. The presence of strong and numerous resonance interactions of different types requires that a large number of resonance interaction parameters is taken into account. Accordingly, in total 24-resonance interaction parameters were varied in addition to those belonging to the diagonal blocks. The final parameters obtained in the fit are presented in columns 3 and 4 of Table 2, and in Table 3, together with their 1σ statistical confidence intervals. The parameters of diagonal blocks given without confidence intervals were fixed as mentioned above. Column 2 of Table 2 reports, for comparison, the values of rotational and centrifugal distortion parameters

Table 1
Statistical information on the ν_1 and ν_3 bands of the AsD_3 molecule

Band	Center	Number of transitions	Number of levels	$J^{\mathrm{upper}}_{\mathrm{max.}}$	$K^{\mathrm{upper}}_{\mathrm{max.}}$	m_1[a]	m_2[a]	m_3[a]
1	2	3	4	5	6	7	8	9
ν_1	1523.2007	850	353	26	23	49.9	33.7	16.4
ν_3	1533.7653	2450	876	28	24	69.1	22.0	8.9

[a] Here m_1, m_2, and m_3 are the percentages of upper energies for which differences $\delta_i = E^{\mathrm{exp}} - E^{\mathrm{calc}}$ satisfy the conditions $\delta_1 \leq 1\times10^{-4}$ cm^{-1}, 1×10^{-4} cm^{-1} $< \delta_2 \leq 3\times10^{-4}$ cm^{-1}, and 3×10^{-4} cm^{-1} $< \delta_3$, respectively.

of the ground vibrational state. The correlation of corresponding parameters for the three vibrational states as evident from Table 2 is fully satisfactory.

The upper state energies were used in the fit procedure with equal weights with the exception of those energies, which were obtained from only one allowed or perturbation-allowed experimental transition. Those energies are presented inTables SM1 and SM2 without experimental uncertainties. The weights of such levels were taken to be zero. Finally, 1229 upper energies gathered in Tables SM1 and SM2 (of which 1131 were used in the fit and 98 ‘zero weighted’) were reproduced with the set of 50 parameters obtained from the fit with an *rms* deviation of 0.00024 cm^{-1}. Columns 4 of Tables SM1 and SM2 reporting the values δ, in units of 10^{-4} cm^{-1}, of the differences between experimental upper energies and the corresponding calculated ones obtained with the parameters gathered in Tables 2 and 3 illustrate the reproductive power of the derived molecular constants. Some more statistical information concerning the investigated bands can be found in Table 1.

A further remark should be made here. From Table SM1 it is evident that, beginning with $J=15$, levels with the value of the quantum number $K=3$ are missing in the list although in the experimental spectrum the corresponding lines are strong both in the *R*- and *P*-branches of the ν_1 band. The reason for omitting these levels is the following. For values $J \geq 15$–16, the splittings of $[J\ K=3\ a_1]/[J\ K=3\ a_2]$ levels in the ground vibrational state reach the order of 0.007–0.008 cm^{-1} and grow with increasing *J* value. At the same time, the $P_3(J)$ and $R_3(J)$ lines in the experimental spectrum are unsplit even for value as large as $J \sim 26$–27. This observation leads to the conclusion that the values of differences between the $[J\ K=3\ a_1]$ and $[J\ K=3\ a_2]$ levels are practically the same both in the ground and in the (1000) vibrational states. On the other hand, experimental line splittings in the *Q*-branch should be about two times larger than the corresponding energy splittings in the ground vibrational state. Indeed, for the states with $J^{\mathrm{upper}}=13$ and 14 such splittings of the expected size were observed in the spectrum, and corresponding energy splittings were calculated and reported in Table SM1. Unfortunately, *Q*-branch lines reaching the above-mentioned states with $J^{\mathrm{upper}}=13$ and 14 are already extremely weak. Regrettedly lines with $[J^{\mathrm{upper}}K=3a_1]/[J^{\mathrm{upper}}K=3a_2] (J \geq 15)$ were too weak in our spectrum to be detectable at all. Taking into account the mutual blending of the lines in the *P*- and *R*-branches, we preferred not to use them in the numerical analysis. For the same reason we did not use in the analysis energies of the states $[J^{\mathrm{upper}}K=1e]$ and $[J^{\mathrm{upper}}K=0a_\lambda]$ ($\lambda=1$, 2 for J^{upper} even and/or odd, respectively).

Inspection of the results evidences that the reproduction of the observations worsens as *J* exceeds 25–26. This fact may be due to two possible reasons. One is the vanishing intensity of the respective transitions. The other possibility has its origin in the failure of the Hamiltonian model to consider resonance interactions with first overtone and combinational levels of bending vibrational states, which are located at lower energies than the stretching vibrational states.

It should be mentioned also that the presence of strong Coriolis interaction leads to appearance of resolved a_1/a_2 experimental splittings not only for the ro-vibrational states

Table 2
Parameters of diagonal blocks of AsD_3 (in cm^{-1})

Parameter	Ground state[a]	(1000, A_1)	(0010, E)
E	–	1523.2005819(745)	1533.7654971(743)
B	1.91724239	1.90390703(434)	1.90384333(427)
C	1.75596416	1.74423397(185)	1.75028993(179)
$D_J\times10^5$	2.470626	2.43649(146)	2.453973(943)
$D_{JK}\times10^5$	−3.09413	−2.95977(113)	−3.07904(107)
$D_K\times10^5$	2.7286	2.62530(115)	2.73368(103)
$H_J\times10^9$	0.8166	0.6521(281)	0.6521[b]
$H_{JK}\times10^9$	−1.4474	−1.0930(425)	−1.0930[b]
$H_{KJ}\times10^9$	0.667	0.6368(596)	0.6368[b]
$H_K\times10^9$	0.76	0.6214(310)	0.6214[b]
$L_J\times10^{13}$	0.0	1.467(193)	1.467[b]
$\varepsilon'\times10^6$	±5.4255	±5.4254(249)	±5.4254[b]
$\varepsilon'_J\times10^9$	∓0.4867	∓0.4867[c]	∓0.4867[c]
$\varepsilon'_K\times10^9$	±0.300	±0.300[c]	±0.300[c]

Parameter	(0010, E)	Parameter	(0010, E)
$2C\zeta$	0.01142292(605)	$\beta\times10^2$	−0.190330(914)
$\eta_J\times10^4$	−0.1162(195)	$\beta_K\times10^7$	0.3831(928)
$\eta_K\times10^4$	0.2489(201)	$\gamma\times10^3$	−0.384342(973)
$\eta_{JJJ}\times10^{12}$	6.234(104)	$\gamma_J\times10^7$	0.3521(199)

Values in parentheses are 1σ statistical confidence intervals in units of the last digit.

[a] Reproduced from Ref. [16], model B with $J_{\mathrm{max.}}=30$.

[b] Set equal to the value of the (1000) vibrational state.

[c] Constrained to the value of corresponding parameter of the ground vibrational state.

Table 3
Parameters of the ν_1/ν_3 Resonance Interaction of AsD_3 (in cm^{-1})

Parameter	Value	Parameter	Value	Parameter	Value
$\alpha^* \times 10^2$	2.8548(192)	$\alpha_J^* \times 10^5$	−0.1832(312)	$\alpha_K^* \times 10^5$	0.770(106)
$\alpha_{JK}^* \times 10^8$	−0.3273(987)	$\alpha_{KK}^* \times 10^8$	−0.922(101)	$\alpha_{JJK}^* \times 10^{11}$	1.122(106)
		$\alpha_{JKK}^* \times 10^{11}$	0.894(136)		
$\beta^* \times 10^3$	2.8968(108)	$\beta_K^* \times 10^6$	−0.2994(283)	$\beta_{JJ}^* \times 10^9$	−0.1051(103)
		$\beta_{JK}^* \times 10^9$	0.5162(175)		
$\gamma^* \times 10^2$	0.272329(431)	$\gamma_J^* \times 10^5$	−0.012783(397)	$\gamma_K^* \times 10^5$	−0.03176(266)
$\gamma_{JK}^* \times 10^8$	0.11534(773)	$\gamma_{JJK}^* \times 10^{11}$	−0.11966(626)		
$\kappa^* \times 10^7$	−0.1921(574)	$\kappa_J^* \times 10^9$	0.08785(995)	$\kappa_K^* \times 10^9$	2.2726(985)
		$\kappa_{JK}^* \times 10^{11}$	−0.3532(287)		
$\theta^* \times 10^7$	0.1219(146)	$\theta_J^* \times 10^{10}$	−0.1450(194)	$\theta_K^* \times 10^{10}$	0.7856(994)
		$\theta_{JK}^* \times 10^{13}$	−1.300(139)		

Values in parentheses are the 1σ statistical confidence intervals in units of the last digit.

with the value of quantum number $K=1$, 2, and/or 3, but also for $K=4$, and 5 (see Table SM2).

By means of band contour simulations we have determined the transition moment ratio $|\mu_1{:}\mu_3|$ to be 1.2 ± 0.05, see Fig. 3. The sign of the intensity perturbation $\mu_1 \zeta_{13}^y \mu_3$ was found to be negative.

6. Equilibrium structure of the AsD_3 molecule

In this section we report on the equilibrium structure of the AsD_3 molecule using the present experimental infrared data and the parameters determined in Ref. [16]. It is well known [21] that in the Born–Oppenheimer approximation the equilibrium bond lengths and equilibrium interbond angles (in our case the As–D bond length $r^e_{\text{As–D}}$ and the D–As–D interbond angle $\alpha^e_{\text{D–As–D}}$) can be derived on the basis of the general formula (9)

$$B_\beta^{(v_1\ldots v_n,\ldots)} = B_\beta^{\text{eq.}} - \sum_\lambda \alpha_\beta^\lambda \left(v_\lambda + \frac{d_\lambda}{2} \right) + \sum_{\lambda\mu} \gamma_\beta^{\lambda\mu} \left(v_\lambda + \frac{d_\lambda}{2} \right) \left(v_\mu + \frac{d_\mu}{2} \right) + \ldots \tag{9}$$

Here B_β^{eq} are the equilibrium rotational constants; α_β^λ and $\gamma_\beta^{\lambda\mu}$ are the rotational–vibrational coefficients which describe the vibrational dependencies of rotational parameters; v_λ and d_λ are the vibrational quantum numbers. Moreover, $d_\lambda=1$ stands for nondegenerate vibrational states, and $d_\lambda=2$ for doubly degenerate ones.

In formula (9) the coefficients α_β^λ are small in comparison with the values of the rotational parameters $B_\beta^{\text{eq.}}$, namely, $\alpha_\beta^\lambda \sim \kappa^2 \times B_\beta^{\text{eq.}}$. Here κ is the small Born–Oppenheimer parameter [21], which in our case has the value of 0.084–0.085. In turn the $\gamma_\beta^{\lambda\mu}$ coefficients are small compared with the α_β^λ values ($\gamma_\beta^{\lambda\mu} \sim \kappa^2 \times \alpha_\beta^\lambda$).

The parameters $B_\beta^{\text{eq.}}$ are connected with the equilibrium moments of inertia by the simple formula

$$B_\beta^{\text{eq.}} = h/(8\pi^2 c I_{\beta\beta}^{\text{eq.}}), \tag{10}$$

and, in turn, the equilibrium moments of inertia $I_{\beta\beta}^{\text{eq.}}$ for pyramidal-type XY_3 molecules can be expressed in the form

$$I_{xx}^{\text{eq.}} = I_{yy}^{\text{eq.}} = r_e^2 \frac{m}{3m+M} [M(1 + 2\cos\alpha_e) + (3m+M)(1 - \cos\alpha_e)] \tag{11}$$

and

$$I_{zz}^{\text{eq.}} = 2mr_{\text{e}}^2(1 - \cos\alpha_{\text{e}}). \tag{12}$$

Evidently the two Eqs. (11) and (12) are sufficient to determine the two equilibrium structural parameters $r^{\text{e}}_{\text{As–D}}$ and $\alpha^{\text{e}}_{\text{D–As–D}}$ if the values of the parameters $I_{xx}^{\text{eq.}}$ (or $B_x^{\text{eq.}}$) and $I_{zz}^{\text{eq.}}$ (or $B_z^{\text{eq.}}$) are known. Neglecting the last term in formula (9) the required parameters $B_\beta^{\text{eq.}}$ can be easily obtained therewith from experimental values of the rotational parameters of the ground vibrational state and the four fundamental vibrational bands. We have taken the required rotational parameters from Ref. [16] and from Table 2 of the present work (see Table 4). The values of the equilibrium bond length $r^{\text{e}}_{\text{As–D}}$ and the interbond angle $\alpha^{\text{e}}_{\text{D–As–D}}$ obtained in this manner are given in the second column of Table 4. The numerical value for Planck's constant was taken from Ref. [23] and for the atomic masses M and m from Ref. [24]. We have not taken into account electronic effects, i.e. the fact that the center of mass of the valence electrons does not coincide with that of the core nuclei.

The third column of Table 4 shows, for comparison, the corresponding and analogously obtained, but significantly less accurate results for the 'mother' species AsH_3. The experimental values of the rotational parameters of the ground state and for the four fundamental bands of the AsH_3 molecule were taken from Refs. [25–27].

Comparison of the values of r^e and α^e parameters for the two species reveals perfect consistency within one of their standard deviations. Comparison may also be made with formerly determined [14], but much less accurate values, $r^{\text{e}}_{\text{As–H}} = 1.513(2)$ A and $\alpha^{\text{e}}_{\text{H–As–H}} = 92.08(7)°$, and with the 'ground state' values $r^0_{\text{As–H}} = 1.520143(4)$ A

Table 4
Rotational state parameters (in cm^{-1}) and equilibrium structures of AsD_3 and AsH_3

State	AsD_3		AsH_3	
	B	*C*	*B*	*C*
(0000)	1.9172424(3)[a]	1.7559642(7)[a]	3.75161458(15)[b]	3.49855548(73)[b]
(1000)	1.9039070(43)[c]	1.7442340(19)[c]	3.715022(73)[d]	3.465920(157)[d]
(0100)	1.9005100(140)[a]	1.7662687(5)[a]	3.74495647(18)[e]	3.52652536(66)[e]
(0010)	1.9038433(43)[c]	1.7502899(18)[c]	3.714171(98)[d]	3.482229(101)[d]
(0001)	1.9282622(28)[a]	1.7497792(4)[a]	3.76272510(47)[e]	3.48078404(67)[e]
$X^{eq.f}$	1.9346556(290)	1.7685363(24)	3.799573(104)	3.534984(128)
α_e		92.0775(40)°		92.0690(80)°
r_e		1.51130(11)Å		1.51101(38)Å

[a] From [16], see Table 2.
[b] From Table 2 of the present paper.
[c] From [25].
[d] From [26].
[e] From [27].
[f] $X^{eq.} = B^{eq.}$ or $C^{eq.}$.

and $\alpha^{e}_{H\text{–}As\text{–}H} = 91.9758(1)°$ from [28]. Again consistency of the structural data reported in Table 4 within one standard deviation in noted, and the superiority of the present results becomes obvious. We point out that the values of the equilibrium structural parameters of AsH_3 and AsD_3 should be exactly equal in the frame of the Born–Oppenheimer approximation. Small discrepancies between the values of the equilibrium structural parameters for the two isotopic species can have different origin, and small differences were recently observed for the equilibrium structures of SbH_3 and SbD_3, which are the heavier homologues of AsH_3 and AsD_3 [29].

In spite of the perfect consistency found for the two-arsine isotopic species we nevertheless have to examine critically systematic errors affecting the correctness of the equilibrium structural parameters and conceivable discrepancies for different isotopic species.

1. One error source may be the neglect of the last term in formula (9) when calculating the $B_x^{eq.} = B_y^{eq.}$ and $B_z^{eq.}$ values. However, it is known from general vibration-rotation theory [21] that the values of the coefficients $\gamma_\beta^{\lambda\mu}$ are very small and of the order κ^4 in comparison to $B_\beta^{eq.}$. Therefore the corrections due to the $\gamma_\beta^{\lambda\mu}$ coefficients should be of the order $B_\beta^{eq.}/10000$.
2. A second reason may be the neglect of nonadiabatic effects. However, according to [21] such effects are responsible for errors of the same κ^4 order.
3. A third conceivable source for systematic errors may be the presence of ambiguities in the effective rotational Hamiltonian used in the analysis of rotation–vibration spectra. It is well known that such ambiguities can arise from the correlation of parameters appearing in the diagonal blocks of the Hamiltonian matrix with resonance interaction parameters occurring in the nondiagonal part of the effective ro-vibrational Hamiltonian (see, e.g. [22,30,31]). Indeed the α-values entering into the calculation of the equilibrium rotational parameters, see, e.g. (9), strongly depend on the chosen reduction of the ro-vibrational Hamiltonian, in particular in the presence of strong Coriolis resonance interactions as in the present case. Such a dependence of the α parameters was, e.g. established for the strongly Coriolis-coupled ν_2/ν_4 dyad of AsD_3 [16] and BiH_3 [10]. There are however linear combinations which even in the presence of strong Coriolis resonance interactions are independent of the chosen reduction [32], and one such reduction-invariant parameter sum is $1/2(\alpha_s + 2\alpha_t)$, i.e. $1/2(\alpha_1 + 2\alpha_3)$ and $1/2(\alpha_2 + 2\alpha_4)$. It is exactly this reduction-invariant sum, which appears in formula (9). Therefore the effects of Coriolis resonance interactions on the vibrational corrections of the rotational parameters cancel, and hence they can be ruled out as sources for substantial systematic errors of the structural parameters of AsD_3 and AsH_3.
4. One further reason that might be responsible for systematic errors and may account for possible disagreement between equilibrium structural parameters of AsH_3 and AsD_3 is the vibrational dependence of the α parameters entering into the calculation of equilibrium rotational constants according to Eq. (9). This means that the difference between the rotational constants at equilibrium and in the ground vibrational state might not be exactly half that between the vibrational ground and first excited states, which is obtained from experiment, provided these latter values are ‘true’ values and free from systematic errors (e.g. by perturbations). In case we are dealing with ‘true’ α values we estimate the errors introduced in this manner to be at most of the order of a few percent of the α values.
5. Since the values of the ground state parameters of AsH_3 and AsD_3 are apparently unambigous, it must be

> the experimental α values that are responsible for the discussed sources of possible errors. We believe that the experimental values are subject to systematic errors which make them differ from the 'true' parameters on which the calculations using formulas (9)–(12) are based. We see the main reason for conceivable systematic errors of the experimental α values in the inadequacy of the chosen Hamiltonian models for the fit of rotational data associated with the excited stretching states because global effects due to bending overtone and combination states have not been considered. Thus, the effective Hamiltonian is perfectly suited to fit the observations but the resulting effective parameters contain a priori unknown contributions from other vibrational states.

Systematic errors affecting the equilibrium structures of AsH_3 and AsD_3 are therefore provoked by errors related to both isotopic species. From the fact that the rotational parameters of AsH_3 are about twice as large as those of AsD_3 one may conclude that the difference between experimental and 'true' α values and hence the systematic error affecting the equilibrium structural parameters of AsH_3 are larger than for the less unharmonic AsD_3 molecule. A global and simultaneous rovibrational analysis of all polyads up to higher vibrational quantum numbers would be necessary to get hands on unambiguous equilibrium rotational constants and structural parameters. It is therefore appropriate to assign larger-pessimistically ten times larger-uncertainties to the structural parameters than those quoted in Table 4 resulting only from error propagation of statistical errors of the ground and excited vibrational state parameters. In conclusion we nevertheless believe that the excellent agreement of the equilibrium structures of AsH_3 and AsD_3 is not just fortuitous but expresses the high reliability of our experimental structure, which should be close to the 'true' one.

Acknowledgements

We thank the Deutsche Forschungsgemeinschaft for financial support, W. Jerzembeck for the synthesis of the sample and M. Litz for help with the manuscript.

Appendix. Supplementary data

Application 1

Supplementary data

Supplementary data associated with this article can be found, in the online version, at doi:10.1016/j.molstruc.2005.05.054

Tables of Experimental Rovibrational Energy Levels for the (1000, A_1) and (0010, E) Vibrational States of AsD_3.

References

[1] A.T. Tokunaga, R.F. Knacke, S.T. Ridgway, L. Wallace, Astrophys. J. 232 (1979) 603.
[2] R.F. Knacke, S.J. Kim, S.T. Ridgway, A.T. Tokunaga, Astrophys. J. 262 (1982) 388.
[3] K.S. Noll, T.R. Geballe, R.F. Knacke, Astrophys. J. 338 (1989) 71.
[4] P. Drossart, E. Lellouch, B. Bezard, J.-P. Maillard, G. Tarrago, ICARUS 83 (1990) 248.
[5] K.S. Noll, H.P. Larson, ICARUS 89 (1990) 168.
[6] L.-M. Lara, B. Bezard, C.A. Griffith, J.H. Lacy, T. Owen, ICARUS 131 (1998) 317.
[7] O.N. Ulenikov, Yu.B. Yuhnik, E.S. Bekhtereva, N.E. Tyabaeva, H. Bürger, W. Jerzembeck, L. Fusina, J. Mol. Spectrosc. 221 (2003) 250.
[8] J.-X. Cheng, X.-G. Wang, H. Lin, Q.-S. Zhu, Spectrochim. Acta A 54 (1998) 1947.
[9] J. Lummila, T. Lukka, L. Halonen, H. Bürger, O. Polanz, J. Chem. Phys. 104 (1996) 488.
[10] W. Jerzembeck, H. Bürger, J. Breidung, W. Thiel, J. Mol. Spectrosc. 226 (2004) 32.
[11] R.E. Stroup, R.E. Oetjen, E.E. Bell, J. Opt. Soc. Am. 43 (1953) 1096.
[12] G.S. Blevins, A.W. Jache, W. Gordy, Phys. Rev. 97 (1955) 684.
[13] P. Helminger, E.L. Beeson Jr., W. Gordy, Phys. Rev. A 3 (1971) 122.
[14] G.A. McRae, M.C.L. Gerry, M. Wong, I. Ozier, E.A. Cohen, J. Mol. Spectrosc. 123 (1987) 321.
[15] V.M. McConaghie, H.H. Nielsen, Phys. Rev. 75 (1949) 633.
[16] H. Bürger, W. Jerzembeck, H. Ruland, M. Wirtz, Mol. Phys. 98 (2000) 589.
[17] G. Guelachvili, K. Narahari Rao, Handbook of Infrared Standards, Academic Press, San Diego, 1986.
[18] G. Guelachvili and 23 other authors, Pure Appl. Chem. 68 (1996) 193.
[19] O.N. Ulenikov, A.B. Malikova, S. Alanko, M. Koivusaari, R. Anttila, J. Mol. Spectrosc. 179 (1996) 175.
[20] Supplementary data for this article are available on IDEAL (http://www.idealibrary.com).
[21] D. Papoušek, M.R. Aliev, Molecular Vibrational-Rotational Spectra, Elsevier Scientific Publishing Company, Amsterdam, Oxford, New York, 1982.
[22] O.N. Ulenikov, J. Mol. Spectrosc. 119 (1986) 144.
[23] E.R. Williams, R.L. Steiner, D.B. Newell, P.T. Olsen, Phys. Rev. Lett. 81 (1998) 2404.
[24] http://www.searchpaniel.com/index.php/Periodic-table-%28huge%29.
[25] G. Tarrago, V. Dana, J.-Y. Mandin, S. Klee, B.P. Winnewisser, J. Mol. Spectrosc. 178 (1996) 10.
[26] O.N. Ulenikov, A.E. Cheglokov, G.A. Shevchenko, M. Winnewisser, B.P. Winnewisser, J. Mol. Spectrosc. 157 (1993) 141.
[27] G. Spiegl, W.A. Kreiner, J. Mol. Spectrosc. 187 (1998) 142.
[28] Wm. B. Olson, A.G. Maki, R.L. Sams, J. Mol. Spectrosc. 55 (1975) 252.
[29] E. Canè, G. DiLonardo, L. Fusina, W. Jerzembeck, H. Bürger, J. Breidung, W. Thiel, Mol. Phys. 103 (2005) 557.
[30] J.K.G. Watson, in: J.R. Durig (Ed.), Vibrational Spectra and Structure vol. 6, Elsevier Scientific Publishing Company, Amsterdam, 1977, p. 1.
[31] K. Sarka, J. Mol. Spectrosc. 133 (1989) 461 (151 (1992) 534).
[32] K. Sarka, D. Papoušek, J. Demaison, H. Mäder, H. Harder, in: D. Papoušek (Ed.), Advanced Series in Physical Chemistry Vibration–Rotation Spectroscopy and Molecular Dynamics vol. 9, World Scientific, Singapore, 1997.